

COMMON PRESSURE VESSEL Ni/H₂ BATTERY — A DEMONSTRATION OF FEASIBILITY

G L HOLLECK*, V FEIMAN and D H LONGENDORFER

EIC Laboratories, Inc , 67 Chapel Street, Newton, MA 02158 (U S A)

Summary

Attractive higher voltage Ni/H₂ batteries can be constructed by connecting several unit cell stacks in series within a common pressure vessel. The practical implementation of this concept requires the complete elimination of electrolyte shunts between unit stacks. To achieve this we have developed a battery design using non-sealing, hydrophobic, thin wall envelopes around each unit stack. The effectiveness of this approach was demonstrated by construction and testing of prototype batteries of about 50 W h, containing up to five unit stacks in series. The batteries successfully completed up to 7000 cycles of a near earth orbit test regime with deep discharge.

Introduction

The development of Ni/H₂ cells began more than a decade ago and was directed primarily towards an improved spacecraft power supply. Although the technology has been considered for various terrestrial uses its only immediate application is in satellites. Here, the advantages of long cycle and calendar life, insensitivity to overcharge and overdischarge coupled with easy state-of-charge monitoring, are of premium value.

Actual applications almost invariably require higher voltage batteries. It has been recognized early on that Ni/H₂ cell stacks can be connected in series within a common pressure vessel (CPV) [1 - 3]. Such battery modules would offer increased gravimetric and volumetric energy density and also a significant reduction in fabrication cost over a series of individual pressure vessel (IPV) cells. Practical implementation of CPV concepts have, however, not been successful. The primary difficulty resulted from the need to completely eliminate electrolyte shunts between the series-connected stacks. Their presence would lead, not only to increased self discharge but also, *via* KOH transference, to imbalance in concentration and distribution of electrolyte between the unit stacks.

*Present address EIC Laboratories, Inc , 11 Dawney Street, Norwood, MA 02062, U S A

To overcome these difficulties we developed a common pressure vessel N_1/H_2 battery design which has been described previously and which addresses all important requirements [4, 5]

- (a) No electrolyte bridging.
- (b) Independent electrolyte management for each unit stack.
- (c) Independent oxygen management for each unit stack
- (d) Good heat dissipation.
- (e) Mechanically sound and practical interconnection.
- (f) Maximum commonality of components and hardware with state-of-

the-art IPV technology

The battery consists of a series arrangement of unit stacks, each in its own plastic cup. Electrolyte, oxygen, and thermal management are handled independently for each unit stack using a single electrode arrangement with electrolyte recirculation and electrolyte reservoir. Narrow hydrophobic channels between unit stacks provide for free gas flow while preventing electrolyte bridging.

In this paper we report on experiments and results which demonstrate the effectiveness of our solutions and show the feasibility of the CPV N_1/H_2 battery concept.

Experimental

Individual N_1/H_2 cell stacks were assembled from standard IPV cell components as shown schematically in Fig 1. The annular nickel oxide electrodes were electrochemically impregnated, slurry-coated nickel plaques with 8.43 cm o.d., 3.17 cm i.d. and 0.08 cm thickness. The hydrogen electrodes consisted of Teflon-bonded platinum black (10 mg Pt/cm^2) with a

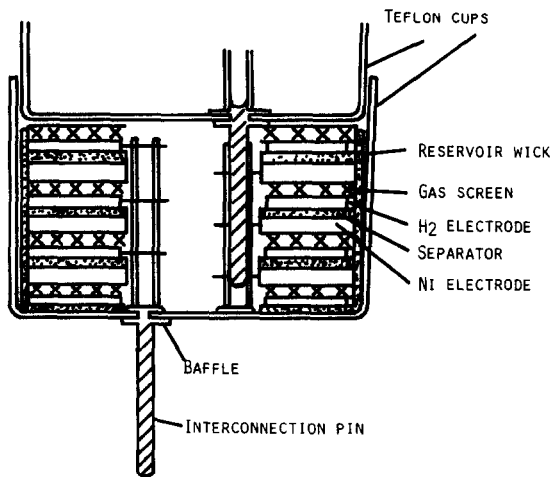


Fig 1 Schematic illustration of unit stack construction for CPV N_1/H_2 battery modules

hydrophobic backing on a current collector mesh. The overall thickness was 0.025 cm. The separators were fuel cell grade asbestos mats (0.025 cm and 0.05 cm thickness from Quin-T Corp.) Various materials, including non-woven nylon (Pellon 2505), non-woven polypropylene (RAI Permion A-1266, Pellon FT-2106, FT-2107), and asbestos were used as reservoir and wick components.

Unit stacks consisting of ten electrode pairs were assembled, essentially as shown in Fig. 1, with nickel pin interconnecting bus members and enclosed in a thin-wall Teflon cup. The cups were obtained by vacuum forming of 0.05 cm thick FEP sheet. The cups served also as alignment and retaining members making an inner core superfluous. These unit stacks represented fairly sturdy subassemblies.

Individual unit stacks were plugged into each other to form a battery stack with series connected cells. The following cups would fit snugly into the rim of the previous cup, thus forming a non-sealing but close fitting cover. Prior to final assembly we attached sensing leads to each stack to allow measurement of individual stack voltages. Our test batteries contained, typically, 3 - 5 series connected unit stacks.

Figure 2 is a schematic diagram of the thick-wall laboratory pressure vessel and the mounting of the stacks. The entire battery stack was held under compression between two end plates. In addition to battery and cell voltage we also monitored gas pressure and, occasionally, temperature from several internal thermocouples.

The standard test regime involved battery discharge for 35 min to 80% DOD followed by 55 min charge including 5 - 10% overcharge. Battery testing as performed at constant current and current values were based on actual capacities delivered during early characterization cycles. The battery cycler was designed in-house. Voltage and pressure data were recorded and processed with Bascom-Turner Electronic Recorders. Periodically the batteries were discharged beyond the 35 min to a voltage cutoff of 1 V per unit stack. Subsequently the battery discharge was continued at 2 A, corresponding approximately to the $C/5$ rate, to ~ 0.5 to 0.75 V per stack. This procedure resulted in the "high rate" capacity of the battery to 1 V and, with the additional capacity at the lower rate, the "total capacity" of each unit stack. When the battery capacity decreased during testing to less than 80% of its original value, the current would be reduced just enough to prevent open circuit periods on discharge. This means the battery would be operated at 100% of its then actual capacity.

In addition to these general conditions, specific cycle regimes were employed in some cases. Generally measured parameters included battery and unit stack voltages, battery pressure, battery capacity, stack capacities and, periodically, stack-pressure vessel temperature differences.

Cycle testing was conducted at 20 °C, maintained by circulating water through external copper coils around the pressure vessel. Battery orientation was varied to examine possible effects of cup orientation with respect to the gravity field. Batteries 7 and 10 were cycled mostly inverted (cup openings facing down).

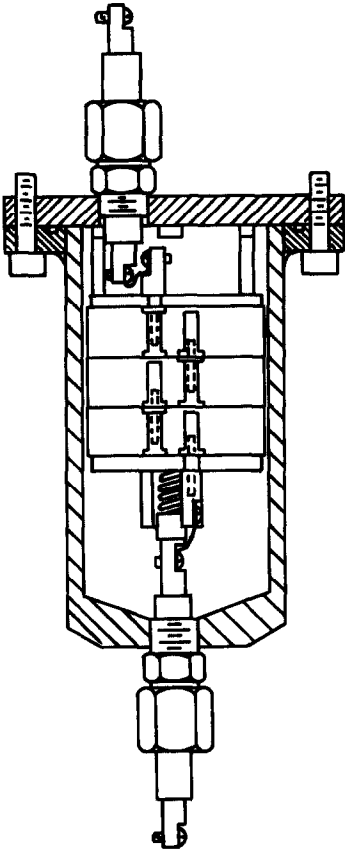


Fig 2 Illustration of laboratory pressure vessel and battery stack mounting.

Low rate current shunts would not be readily noticeable during high rate cycling, and thus we conducted a special test for this condition. It consisted of extended open circuit stand after full charge with subsequent complete discharge as described above. A shunt load across the entire battery would increase the apparent rate of self discharge, and a shunt load between a group of unit stacks would lead to a relative shift in remaining unit stack capacities.

Batteries 3 - 6 were activated by measuring a predetermined amount of electrolyte (30% KOH) into each cup prior to insertion of the battery stack into the pressure vessel. This was followed by a time for electrolyte equilibration under vacuum prior to pressurization with hydrogen to 16 atm.

Batteries 7 - 10 were vacuum impregnated by the following sequence: evacuation of the assembled battery, back filling with 30% KOH, equilibration, draining of excess KOH *via* repeated pressurization with H_2 , charging in inverted position, draining of KOH.

After extended cycle testing, the batteries were disassembled for examination of changes in components and for analyses of the amount and concentration of electrolyte in each stack and in the pressure vessel

Results and discussion

Batteries 3 - 10 contained 4, 3, 5, 3, 4, 4, 3 and 4 stacks in series, respectively. Batteries 3 - 6 were activated by the addition of a pre-measured quantity of electrolyte into each unit stack. Batteries 7 - 10 were activated by vacuum impregnation of the completed battery module (evacuation and back filling with electrolyte). The former procedure allowed exact control and following of the amount of electrolyte in each unit stack. The pressure vessel was completely dry at the beginning of testing. The second procedure assures full saturation of the accessible pore volume. It also permits complete battery assembly prior to introducing electrolyte and corresponds to present IPV practice.

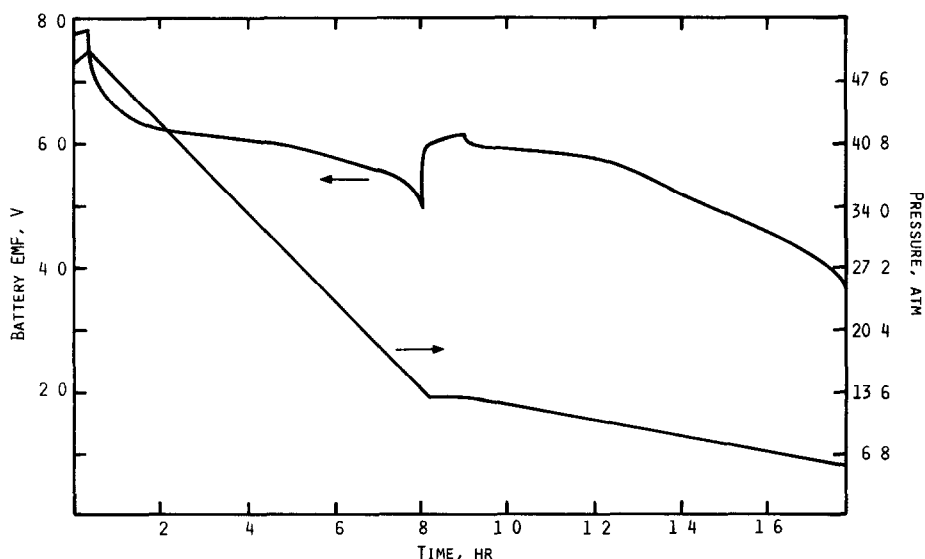


Fig 3 Characteristic voltage and pressure profiles during a complete battery discharge Battery No 5, Cycle 702, discharged at 11.7 A followed by 0.1 h open circuit and further discharge at 2 A

Characteristic changes in battery voltage and hydrogen pressure during the two-stage discharge are shown in Fig. 3. Characteristic voltage-time traces for individual cell stacks are shown in Fig. 4. A voltage inflection, as shown after 35 min of discharge in Fig. 4, was typically observed in the first complete discharge subsequent to extended partial discharge cycling and reflects a "memory effect" in the nickel oxide electrode. Figure 4 also shows

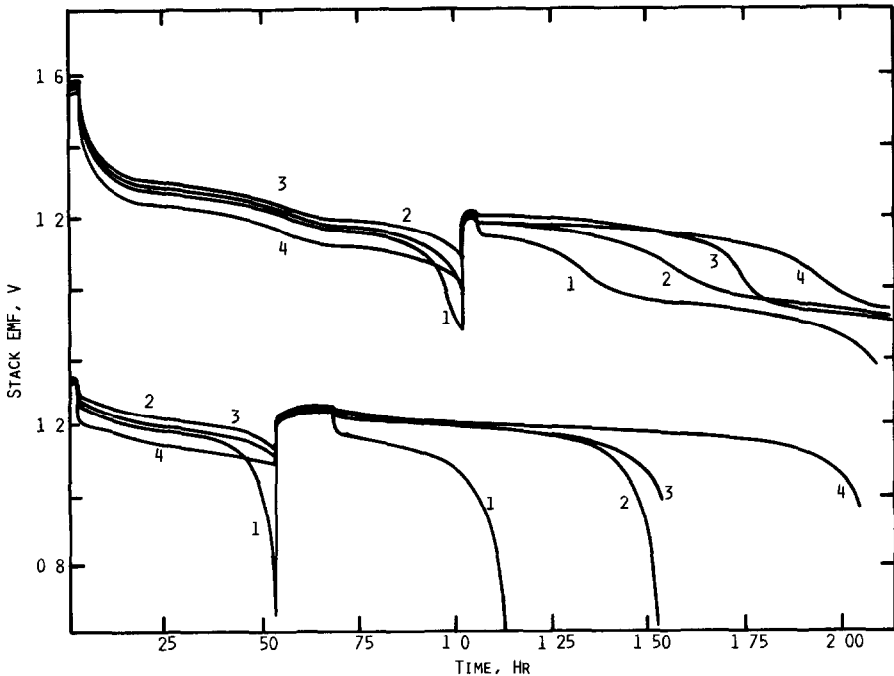


Fig. 4 Voltage profiles of Stacks 1 - 4 during a complete battery discharge during cycle testing (upper traces) and following 1371 h on open circuit stand (lower traces) for Battery No 7, Cycle 1099 Both discharges were at 12.75 A followed after a short open circuit transition by further discharge at 2 A (the voltages of Stack 4 include additional terminal resistance drop)

the same discharge regime applied to the battery after stand for extended time on open circuit. Although the overall capacity is reduced by self-discharge, the capacity distribution between the unit stacks is unchanged, demonstrating the absence of intercell shunt currents

The performance of batteries 3 - 6 was remarkably similar. The capacity change during test cycling is illustrated in Figs. 5 and 6. The high rate capacity during the early phase of cycling was between 8 and 9 A h. This was less than expected based on the measured flooded capacity of the nickel electrodes of 12 and 13 A h. The high rate battery capacity showed a slow decline over approximately 1000 - 2000 cycles. The total capacity changed much less. The main effect was a shift of the high rate capacity to lower values

To determine the role of electrolyte amount and distribution on battery performance we opened the vessel and added further premeasured amounts of electrolyte to the unit stacks. In all cases this resulted in a capacity improvement, the extent and duration of which depended on the relative electrolyte saturation of the stacks. No electrolyte had been lost from the stacks into the pressure vessel. However, due to cathode swelling and opening of previously inaccessible pores, the pore volume available for

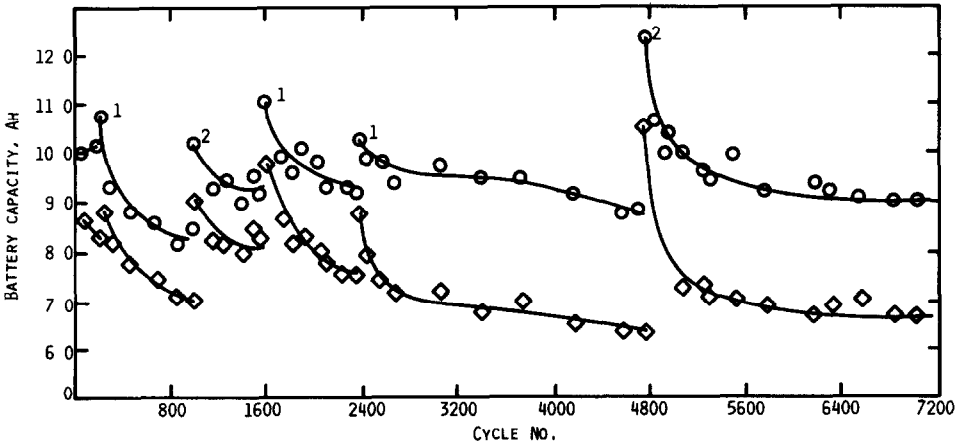


Fig 5 High rate capacity to 1 V (lower curves) and total capacity (upper curves) of Battery No 3 during near earth orbit cycling (1) Extended low rate charge, (2) electrolyte addition

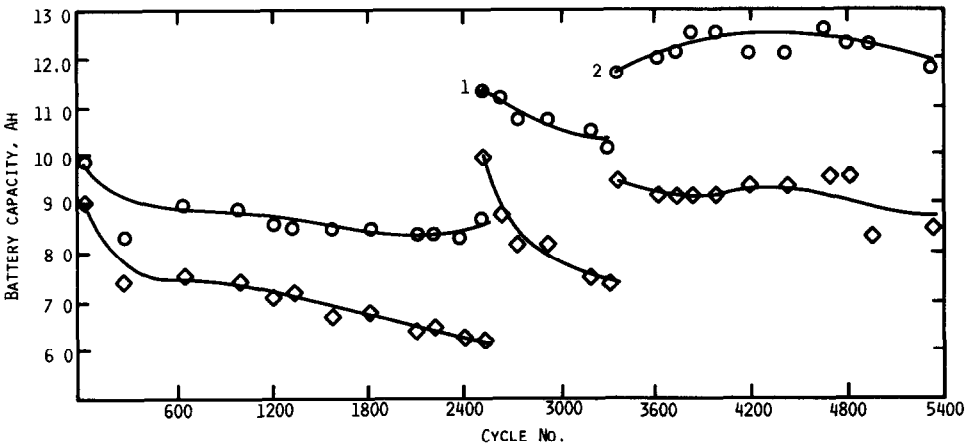


Fig 6 High rate capacity to 1 V (lower curve) and total capacity (upper curves) of Battery No 6 during near earth orbit cycling (1) Electrolyte addition, (2) vacuum impregnation

electrolyte had increased. Temporary improvements were also observed after extended low rate charge. We believe that electrolyte redistribution within the cathode is responsible for this effect. In battery 6 we intentionally operated the unit stacks at different electrolyte saturations. The effect of electrolyte additions is illustrated in Table 1.

Battery modules 7 - 10, which were activated by vacuum impregnation, also showed very consistent behavior. Their capacity during early cycling was higher with 11.5 A h at high rate, 12.5 A h overall for modules 8 - 10 and 12.7 A h at high rate, 14 A h overall for module 7. The overall rate of

TABLE 1

Electrolyte volume and total capacity of the unit stacks in battery 6

Unit stack	Cycle 989		Cycle 3284		Cycle 3612	
	KOH (cm ³)	C (A h)	KOH (cm ³)	C (A h)	KOH* (cm ³)	C (A h)
1	50	9.2	70	12.1	66	11.4
2	45	8.4	50	9.5	59	11.4
3	40	9.3	45	11.3	56	14.2

*Following vacuum impregnation, amount determined by tear down analysis after test

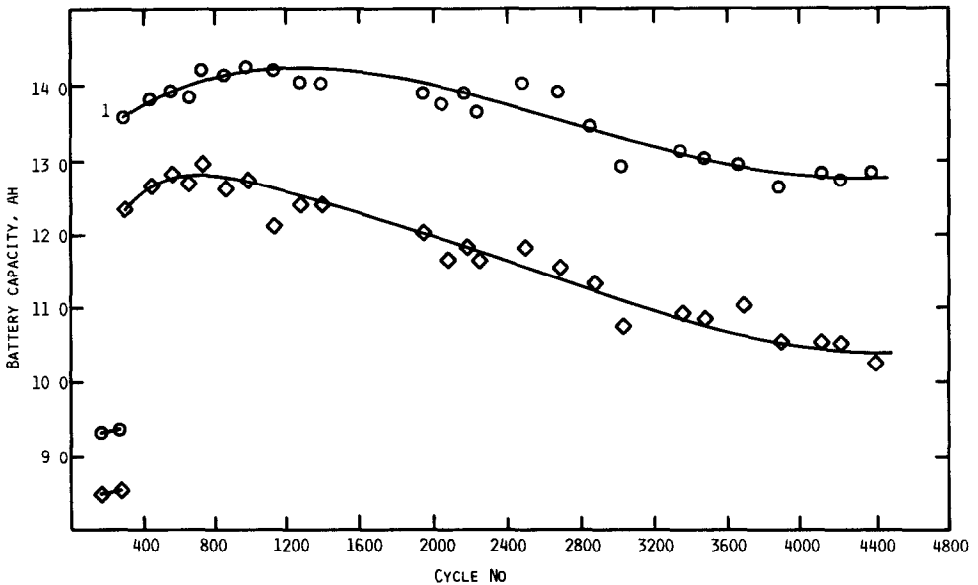


Fig 7 High rate capacity to 1 V (lower line) and total capacity (upper curves) of Battery No. 7 during near earth orbit cycling (1) Vacuum impregnation

capacity decline with cycling was similar for all cells with approximately 4 - 7% per 1000 cycles. The data for battery 7 are shown in Fig. 7.

The observed capacity difference between these groups of batteries does not merely correspond to the overall electrolyte quantity in each stack but also to the procedure of electrolyte introduction. We have observed nickel electrode performance variations as a function of activation procedure in our earlier work on Ni/H₂ and Ni/Cd cells, but generally not to the same extent. The magnitude of the effect may be related to the specific type of Ni electrode employed here. Apparently, careful vacuum impregnation of the electrode structure allows wetting of micro pores in the active material which are not readily accessible by mere capillary action. Later vacuum impregnation of group one modules resulted in capacity improvement in

those batteries which had not yet been extensively cycled, but was relatively inconsequential in high cycle number modules

Periodically throughout the test cycle, periods of open circuit stand were used to probe for possible electrolyte shunts. Invariably, even after vacuum impregnation, the relative capacities of the individual stacks were unchanged after a 100 h stand, proving the absence of any electrolyte shunts. This is highly significant because electrolyte shunts would not only lead to imbalance between stacks and a loss in energy efficiency but would also result in continued unidirectional transfer of KOH from one stack into another *via* ion migration. In the electrolyte shunt the current is carried by OH^- and K^+ ions which move in the electric field according to their transport numbers of 0.78 and 0.22, respectively (30% KOH). Assuming a cation solvation complex with two water molecules, and neglecting re-equilibration by diffusion, we calculate the transfer of 0.46 g of KOH/A h and 0.37 g of H_2O /A h in the direction of the current flow. This transfer is unidirectional, independent of whether the battery is charged or discharged, and therefore has to be prevented if long lifetimes are required. The ultimate problem results from flooding and drying of the respective stacks since water transport through the vapor phase will tend to equalize electrolyte concentrations.

The periods on open circuit stand were also used to measure battery self discharge. We have shown in earlier investigations [6] that the self discharge rate is proportional to hydrogen pressure. This results in an exponential decrease of remaining capacity. The measured rate constants determined from the plots of $\log P_{\text{H}_2}$ vs time (after an initial time of about 20 h such plots are linear) are summarized in Table 2. The values agree with those found in IPV Ni/H_2 cells. The data show also that the rate of self discharge decreases with increasing cycle number, indicating changes in the reactivity of the active nickel oxyhydroxide with hydrogen.

Tear down analyses of the batteries confirmed a swelling and blistering of the nickel electrodes after extended cycling. This increase in pore volume has, in turn, a disturbing effect on the electrolyte balance within the stacks. The intrinsic capacities of the nickel electrodes (measured flooded) had not changed significantly after the cycle test. Electrolyte loss from the unit stacks into the pressure vessel was effectively prevented by the cup enclosure, irrespective of battery orientation. This was demonstrated by extended operation in the inverted orientation (cup openings facing down). Tear down analysis of earlier cells revealed localized heat damage to gas screen and occasionally holes in the Teflon cups resulting from oxygen-rich gas bubbles. This problem was successfully solved by modifications in stack construction. Up to 4000% overcharge at the C rate (44 h) without drying or O_2 damage demonstrated the ruggedness of our CPV design.

Potential long term changes in electrolyte were further explored by mathematical modeling of the pertinent transport phenomena. Water vapor leaving the cups during H_2 evolution is fully recovered during discharge. In fact, the equilibrium water vapor pressure in the pressure vessel after

TABLE 2

CPV Ni/H₂ battery self discharge parameters

Derived from $\log p = \log p_0 - \frac{kRT}{2.3 V} t$, $k_1 = \frac{k}{n}$, where $p = \text{H}_2$ pressure, $R = \text{gas constant}$,
 $T = \text{temperature, } ^\circ\text{K}$, $V = \text{free vessel volume}$, $t = \text{time}$

Battery number	n No of stacks	Cycle no	Battery constant, k (mol h ⁻¹ atm ⁻¹)	Unit stack constant, k_1 (mol h ⁻¹ atm ⁻¹)
3	4	638	1.58×10^{-4}	3.95×10^{-5}
		3504	6.71×10^{-5}	1.67×10^{-5}
4	3	1973	5.21×10^{-5}	1.74×10^{-5}
5	5	110	1.44×10^{-4}	2.9×10^{-5}
		529	1.21×10^{-4}	2.4×10^{-5}
		2658	8.3×10^{-5}	1.66×10^{-5}
5	3	5019	5.2×10^{-5}	1.7×10^{-5}
		5068	4.7×10^{-5}	1.6×10^{-5}
6	3	1223	8.71×10^{-5}	2.9×10^{-5}
		3964	4.8×10^{-5}	1.6×10^{-5}
7	4	61	1.1×10^{-4}	2.75×10^{-5}
		1099	5.7×10^{-5}	1.44×10^{-5}
		2252	5.9×10^{-5}	1.5×10^{-5}
		3768	5.5×10^{-5}	1.37×10^{-5}
8	4	886	7.9×10^{-5}	2.0×10^{-5}
9	3	80	4.6×10^{-5}	1.5×10^{-5}
10	4	592	7.8×10^{-5}	2.0×10^{-5}

discharge is lower than during idle stand. A moderate increase in the H₂ precharge pressure greatly decreases the amount of water vapor movement and prevents temporary water condensation in the pressure vessel. Recently, we have extended our mathematical model to predict the extent and rate of electrolyte concentration and volume change for each stack as a function of time and number of cycles if operating parameters (*e.g.*, depth of discharge, stack temperature) are not equal for all stacks. This mathematical model will be published elsewhere. The results predict that moderate stack imbalances do not present a serious problem. Complete malfunction of a stack will no longer lead to electrolyte equilibrium within normal electrolyte volume tolerances. However, the rate of water vapor transfer is slow resulting in a very gradual performance degradation.

In summary, we can conclude that CPV Ni/H₂ batteries are feasible. The cup approach has proven effective in eliminating electrolyte shunts.

Electrolyte balance and oxygen recombination can be managed separately for each unit stack [7] Therefore, there appear to be no fundamental problems precluding implementation of CPV battery modules

Acknowledgements

We thank Dr P O'D. Offenhartz for the mathematical modeling of water transport and the Air Force Wright Aeronautical Laboratories, Aero Propulsion Laboratory, Wright-Patterson AFB, Ohio, for their support under Contract F33615-79-C-2035.

References

- 1 D Warnock, *US Pat 297210* (1976)
- 2 L Swette and J Giner, *US Pat 3990910* (1976)
- 3 G Van Ommering, J F Stockel and J D Dunlop, *US Pat 4115630* (1978)
- 4 G L Holleck, *Proc 15th IECEC*, Am Inst of Aeronautics and Astronautics, Inc , New York, NY, 1980, p 1908
- 5 G L Holleck, *US Pat 4327158* (1982)
- 6 G L Holleck, M J Turchan and D DeBicari, *Proc 28th Power Sources Symp* , The Electrochemical Society, Inc , Princeton, NJ, 1978, p 139
- 7 G L Holleck, *US Pat 4127703* (1978)